Characterization and morphological reconstruction of the Terny impact structure, central Ukraine

V. L. SHARPTON[1*], R. V. KROCHUK[2], and R. R. HERRICK[2]

[1]Lunar and Planetary Institute, 3600 Bay Area Blvd., Houston, Texas 77058, USA
[2]Geophysical Institute, University of Alaska Fairbanks, 903 Koyukuk Dr., Fairbanks, Alaska 99775, USA
[*]Corresponding author. E-mail: sharpton@lpi.usra.edu

Abstract–The Terny impact structure, located in central Ukraine, displays a variety of diagnostic indicators of shock metamorphism, including shatter cones, planar deformation features in quartz, diaplectic glass, selective melting of minerals, and whole rock melting. The structure has been modified by erosion and subsequently buried by recent sediments. Although there are no natural outcrops of the deformed basement rocks within the area, mining exploration has provided surface and subsurface access to the structure, exposing impact melt rocks, shocked parautochthonous target rocks, and allochthonous impact breccias, including impact melt-bearing breccias similar to suevites observed at the Ries structure. We have collected and studied samples from surface and subsurface exposures to a depth of approximately 750 m below the surface. This analysis indicates the Terny crater is centered on geographic coordinates 48.13° N, 33.52° E. The center location and the distribution of shock pressures constrain the transient crater diameter to be no less than approximately 8.4 km. Using widely accepted morphometric scaling relations, we estimate the pre-erosional rim diameter of Terny crater to be approximately 16–19 km, making it close in original size to the well-preserved El'gygytgyn crater in Siberia. Comparison with El'gygytgyn yields useful insights into the original morphology of the Terny crater and indicates that the amount of erosion Terny experienced prior to burial probably does not exceed 320 m.

INTRODUCTION

The Terny (aka Ternovka, Ternovsk, Ternovskaya) impact structure is located in the south-central part of the Ukrainian Shield (Fig. 1), on the northeast outskirts of Krivoy Rog, amidst one of the world's most significant Precambrian iron deposits. Observations made during geological mapping and exploration in the 1960s and 1970s could not be reconciled with the classic geological understanding of the Precambrian basement formations and during the late 1970s an impact origin was proposed (Nikol'sky 1979). Nikol'sky (1991) first estimated the impact age to be Devonian based on a model erosion rate combined with crater size and depth estimates available to him. Later, Val'ter et al. (1981) analyzed feldspars and micas from the target rocks using a K/Ar method and reported a crater age of 280 ± 10 Ma (Late Carboniferous—Early Permian).

Because early work on this structure was available only in Soviet scientific publications, awareness of Terny was late in arriving to the Western literature. The earliest appearance of Terny in a list of terrestrial crater forms came in 1982 (Grieve 1982), although its age, location, and preservation state were not provided and it was inaccurately listed as an impact into sedimentary target rocks. Numerous papers have since mentioned Terny in light of its exploited iron (and uranium) resources (e.g., Grieve and Masaitis 1994; Reimold et al. 2005) and several cursory estimates of its size, precise location, and preservation state have been published (Table 1). Aside from early descriptions in Russian literature (e.g., Nikol'sky et al. 1983; Nikol'sky 1991), however, the observational constraints upon which these estimates rest remain poorly documented. The disparities in location (approximately 25 km in N–S direction if the Reimold et al. estimate is

Fig. 1. Location of the Terny structure. Stippled region indicates general trend of the Ukrainian Shield.

Table 1. Estimates of Terny's basic characteristics.

Location (lat; lon)	Diameter (km)	Erosion level	Reference
Not provided	>6	Considerable	Masaitis et al. (1981)
48.02° N; 33.08° E	8	Not provided	Grieve (1987)
Not provided	8–16	>800 m	Val'ter et al. (1989); Val'ter (1992)
48.02° N; 33.08° E	12	Not provided	Grieve and Shoemaker (1994)
48.02° N; 33.08° E	15	Not provided	Grieve et al. (1995)
48.25° N; 33.5° E	11	Heavy	Masaitis (1999)
48.13° N; 33.52° E	6.5–8	~700	Krochuk and Sharpton (2003)
49.13° N; 33.52° E[a]	11	Not provided	Reimold et al. (2005)
48.13° N; 33.52° E	11	Not provided	Earth Impact Database[b]

[a]Most likely a transcription error.
[b]http://www.passc.net/EarthImpactDatabase/index.html.

interpreted as a transcription error) and diameter (>2×) shown in Table 1 attest to the need for additional research and documentation if the nature and potential of this structure are to be fully exploited.

Beginning in 2002, we undertook an effort to understand this poorly characterized structure by analyzing available geological maps and samples from surface and subsurface localities to constrain the spatial distribution of cardinal impact units and materials. In this article, we summarize this work and use it as a rudimentary basis for estimating Terny's original size, morphology, and current preservation state. In so doing, we address the uncertainties and other challenges faced when attempting reconstructions of this and other eroded relics of impact craters on Earth.

Geological Setting

The impacted rocks are part of a complex 4–6 km wide synform greater than 100 km long, situated between two high-grade metamorphic granitic domes within the Middle-Dniprean tonalite-greenstone complex of the Ukrainian Shield. The relevant characteristics of this stratigraphic section are summarized in Table 2. Lower Proterozoic amphibolites and ultrametamorphic granitoides of the Konksko-Verkhovtsevs'ka suite are the main components of the domes. The syncline itself comprises metamorphic quartzites, jaspilites (hematite-goethite-martite quartzites), chlorite-biotite gneisses, and metacarbonate rocks of the overlying Kryvoriz'ka series. Gneisses of the latest Ingulo-Ingulets'ka series are

Table 2. Target stratigraphy at the Terny structure.

Unit name and related impactite	Unit symbol	Unit age (Ma)	Lithological descriptions (individual members distinguished by semi-colons)

Ingulo-Ingulets'ka Series
  Not represented in Terny
  impactites
	PR$_1$ii	1960 ± 10	Biotite-plagioclase gneisses, schists.

Upper Kryvoriz'ka Series Melt rocks (tagamites)	PR$_1$kr$_3$	2615 ± 15	Magnetite quartzites, metaquartzites, graphite-biotite-quartz schists, marbles and limestones, biotite-microcline-plagioclase paragneisses, meta-sandstones and biotite-quartz schists.

Middle Kryvoriz'ka Series
  Suevite-like melt-bearing breccias
  and tagamites
	PR$_1$kr$_2$		Goethite-hematite-martite quartzites, often replaced with disperse hematite quartzite layers;
			Chlorite schists with magetite-hematite quartzite layers;
			Jaspelite, martite quartzites with schist interlayers;
			Chlorite-biotite-quartz schists with iron quartzites, often with graphite;
			Cummingtonite-biotite-quartz, chlorite-biotite-quartz schists with quartzite interlayers.

Lower Kryvoriz'ka Series
  Suevite inclusions
  Parautothonous rocks
	PR$_1$kr$_1$		Talc-chlorite-carbonaceous schists and acid-amphibole metasomatites formed by these schists, phillite schists, quartz sandstones.

Konksko-Verkhovtsevskaya Series
  Suevite inclusions
  Parautothonous rocks
	PR$_1$kv	2824 ± 20	Amphibolites with in situ ultrametamorphic alskite-aplite granites and microcline granite-gneisses

widely distributed in the area, but absent near Terny. The basement is thinly covered with up to 50 m of recent sediments consisting primarily of clays and sands (Fig. 2).

Representative samples of target formations were isotopically dated by N. P. Shcherbak and his team at the Institute of Geochemistry, Mineralogy and Ore Formation in Kyiv, Ukraine. The location where the samples were collected is about 15–20 km to the north of the impact structure, well outside the range of shock resetting on isotopic systems. The oldest unit, the Konsko-Verkhovtsevs'ka series amphibolites, was dated at 2825 ± 20 Ma using the U/Pb method on zircons (Shcherbak et al. 1984). The age of the East-Annovsky belt, which is correlated to the Kryvoriz'ka Series, is 2615 ± 15 Ma. Rocks from the overlying Ingulo-Ingulets'ka series are 1960 ± 10 Ma (Bibikova et al. 2008)

OBSERVATIONS

Although there are no natural exposures of the basement rocks within the area, the search for exploitable iron deposits prompted an exploration campaign that has resulted in hundreds of drill holes, two major open-pit mines, and a network of subsurface mine tunnels which provide access to rock units to a subsurface depth of 1022 m. A proprietary reconnaissance-level basement map covering the eastern

two thirds of the structure was produced in the 1970s but was never published. This map's utility is somewhat limited because interpretations required to interpolate between widely spaced data points were made prior to recognizing the impact origin of Terny. However, it covers the highly deformed suite of rocks associated with the proposed central uplift as well the outlying floor and wall rocks to the east and south. The time-stratigraphic boundaries shown in Fig. 3 and the locations of mapped lithological units shown in Fig. 4 were taken from this map but unit interpretations have been updated, where possible, to reflect their origin through impact. While we are confident in the interpretations provided, we cannot vouch for the accuracy of the mapped unit boundaries.

Fieldwork and Sampling Strategy

During our field work at Terny we were able to sketch relevant sections of the proprietary map and were granted access to some of the drilling logs within the structure. We were also provided with full access to the open pits and parts of the subsurface mines. We collected representative samples from impact melt and breccia units as well as target rocks shocked to varying degrees to evaluate the regional distribution of peak shock pressures and to assist in reconstructing the original crater morphology.

Fig. 2. Open-pit iron mine near Krivoy Rog taken by an unknown photographer circa 1900. Approximately 25 m of sediments (massive, unconsolidated, rilled) overlie steeply dipping schistose units of the Precambrian Shield. The terrace at the top of the uppermost ladder marks the interface between overburden and crystalline rocks.

The Pervomaysk open pit provides broad access to the deformed basement rocks near the center of the structure as well as vestiges of the outlying impact breccias emplaced on the original, "true" (see Grieve and Robertson 1979) crater floor (Fig. 3). The Annovsk quarry, located at the northern part of the study area, exposes target rocks of the outer crater floor and walls exhibiting impact features indicative of weaker shock pressures. Access to the subsurface is through the Pervomaysk-1 and Pervomaysk-2 (hereafter P1 and P2) mine shafts located north of the Pervomaysk open pit. A system of horizontal mine tunnels ("levels") connect P1 and P2 mine shafts with the United mine shaft located approximately 4 km to the southeast. We traversed and sampled within levels 250 m, 365 m, 520 m, and 750 m between P2 and United. Sample access is discontinuous, however, as level walls are commonly sprayed with gunite to minimize spall and dust.

Distribution of Impactites

Various indicators of an impact origin were reported for this crater during the 1980s and early 1990s. These include shatter cones (Nikol'sky 1979, 1991; Gurov 1982; Val'ter 1992), impact melt glass (Eremenko and Yakovlev 1980; Masaitis et al. 1981; Nikol'sky et al. 1983; Nikol'sky 1991), planar deformation features (PDFs) in quartz grains (i.e., Val'ter et al. 1981; Nikol'sky et al. 1983), diaplectic quartz glass (Mashchak and Orlova 1985), and high-pressure phases such as stishovite (Gurov 1982) and lonsdaleite (Val'ter 1992). Unfortunately few details of this work have made their way into the Western scientific literature.

Melt Rocks

Mordovets (1977) first documented exposures of melt rocks within the Terny structure, although they misidentified these glassy-to-fine-grained, vesiculated rocks, and associated breccias as evidence of Phanerozoic volcanic reactivation of the Ukrainian Shield. However, no other regions of the Ukrainian Shield show similar rock types or any other evidence of reactivation during this time interval. These rocks have been confirmed subsequently as impact melt products based on the presence of diagnostic indications of shock
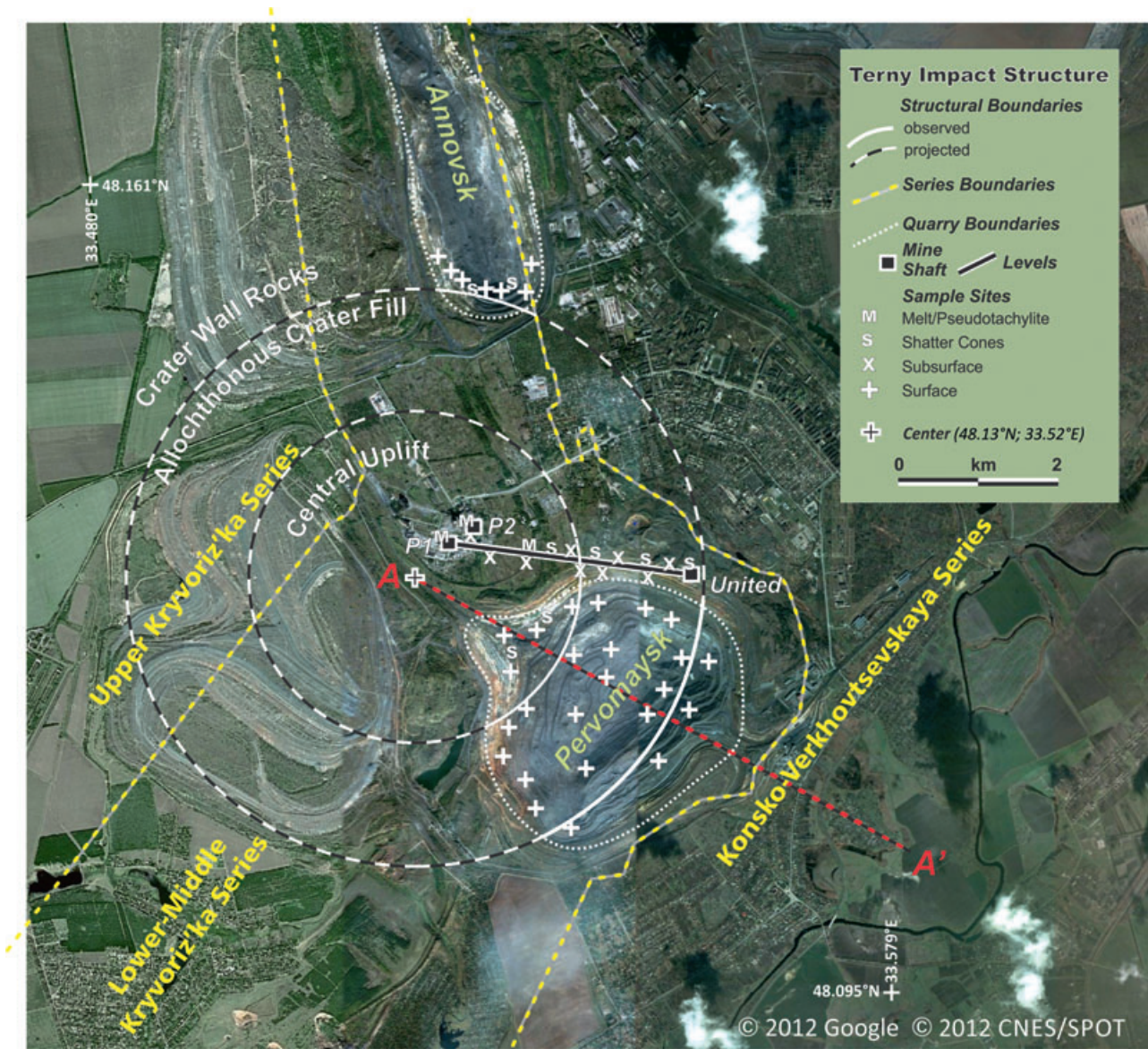
Fig. 3. Color satellite image covering our study area within the buried Terny structure annotated with sample localities, mine sites, Precambrian stratigraphic units, and our interpretation of the structure's major lithological components. P1 and P2 indicate locations of the Pervomaysk-1 and -2 mine shafts, respectively. The line connecting A (proposed crater center) and A' (its estimated original rim) refers to our modeled cross section shown in Fig. 9.

metamorphism (Masaitis et al. 1981) and their unusual compositions. Melt rocks can be divided into two types based on their appearance and composition. Highly ferriferous tagamites or "yurites" (Nikol'sky 1991) are dense, dark-colored rocks with significant primary mafic minerals content (Fig. 5a) derived from the Middle Kryvoriz'ka Series PR_1Kr_2 iron quartzites and schists. The other type of melt rock is light colored and vesiculated with many vugs filled with secondary minerals. The protolith of this type appears to be the metaquartzites and gneisses of the Upper Kryvoriz'ka series PR_1Kr_3 (Fig. 5b).

Previously mapped exposures of melt rock unconformably overlie crystalline basement east of mines P1 and P2 (Figs. 3 and 4). We also observed significant melt-rock exposures in the subsurface to a maximum depth of approximately 400 m, with only uncommon and thinner occurrences in deeper shafts. These melt rocks typically occur in dyke-like exposures of various thicknesses between large (10–100 m) blocks (megablocks). In these larger exposures, we observed a continuum from completely melted rocks near the medial trace of the exposure to melt-matrix breccias (Figs. 5c and 5d) along the margins. Field relations
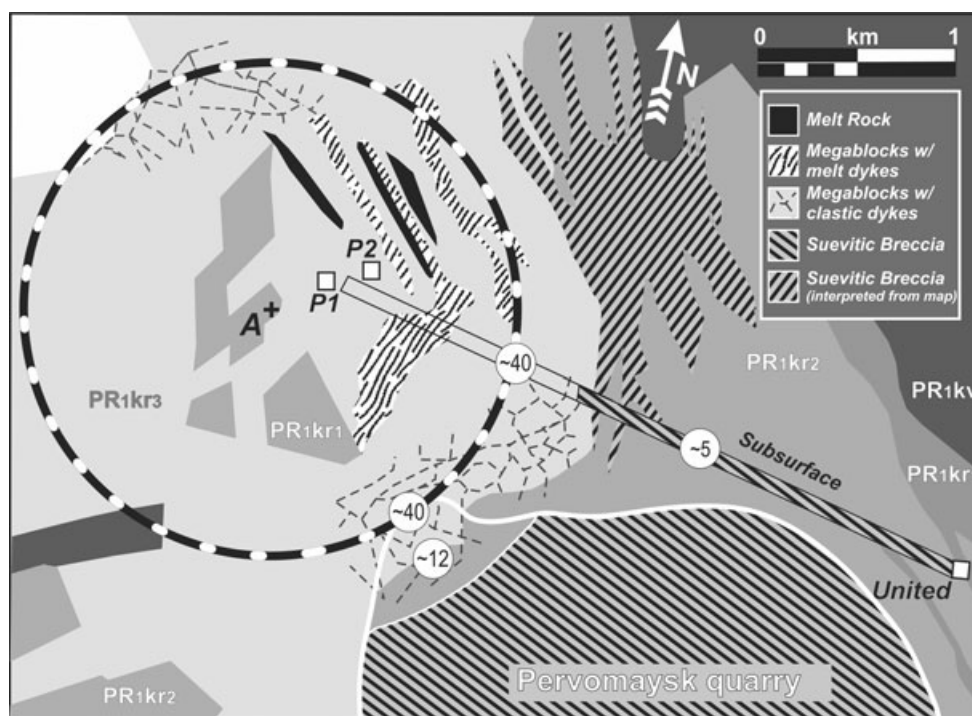
Fig. 4. Sketch map derived from unpublished industrial map updated with our lithological interpretations. Dashed concentric circle denotes outermost limit of samples containing diaplectic quartz glass indicative of approximately 40 GPa shock pressures; outward limit of approximately 12 GPa and approximately 5 GPa pressures, interpreted from PDF orientations are also shown. Estimated crater center is shown by +. Note direction of geographic North.

indicate that the larger melt bodies at shallow levels represent interstitial melt between megablocks and the smaller, deeper dykes are impact melts forcefully injected into the deeper reaches of the central structure.

Aside from melt-rock clasts commonly observed in allochthonous breccia deposits, the impact melt rocks we and others have observed are confined to the zone near P1 and P2 mines that we interpret as the central uplift in Fig. 3.

Allochthonous (Clastic-Matrix) Breccias

Continuous exposures of allochthonous breccia, commonly containing both glass-laden and shatter-cone bearing clasts, form a broad, arc-shaped unit in the central floor of the Peromayskyj pit trending approximately SW–NE and 1.7 km in width (Fig. 3). The subsurface extension of this unit is also observed in the walls of the United mine shaft and along the 365 level westward toward P2 for a distance of approximately 1.5 km where it thins in contact with the subjacent shocked basement rocks of the central uplift. No allochthonous breccias were observed or have been reported in the Annovsk quarry or the northwestern-most portion of the Peromayskyj quarry.

Clasts range in size over seven orders of magnitude from micron-sized particles to megablocks, some as large as 200 m across. Lithic clasts represent the full spectrum of the complex target-rock assemblage and both shatter-coned and shock-melted clasts are common (Fig 5e). We did not observe any aerodynamically sculpted clasts as documented in uppermost "fallback" suevite from the Ries crater in Germany (e.g., von Engelhardt 1997). Furthermore, the deeper exposures of allochthonous breccia between P2 and United appear as discrete patches separating 100–200 m wide zones of parautochthonous target rocks.

With the limited exposures the mines afford, it is not possible to determine with certainty whether this arrangement represents a basal megablock assemblage or allochthonous breccia dykes injected into the subjacent (originally adjacent) wall rocks prior to uplift as previously interpreted (Val'ter and Ryabenko 1982; Krochuk and Sharpton 2003). However, where observable, megablocks separated by finer-grained allochthonous material show broad diversity in composition and orientation, suggesting that they represent true allochthonous blocks rather than the remains of an autochthonous unit intruded by breccia dikes. We therefore provisionally interpret the deep units observed in the walls of level 365 as the base of the allochthonous crater fill deposits (Fig. 3) emplaced within the annular trough located between the central
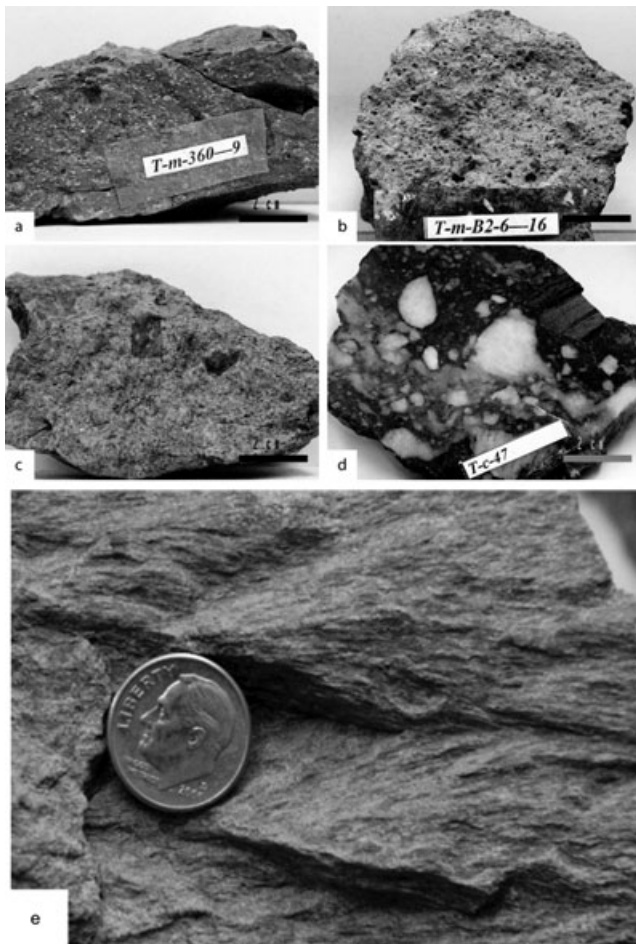
Fig. 5. Impact rocks from Terny impact structure. a) Ferriferous impact melt rock after jaspilite; b) porous impact melt rock representing PR_1kr_3 schist or gneiss; c) impact melt rock (tagamites) with undigested target-rock fragments; d) polymict impact melt breccia. Most fragments are quartzites, dark fragment in the upper right corner is magnetite quartzite; e) Middle Kryvoriz'ka Series schist with a typical shatter cone. Scale bars in a–d are 2 cm long; coin is 17.9 mm in diameter.

uplift and the deformed, originally terraced, target rocks of the distal crater floor and wall.

Distribution of Solid-State Shock Metamorphic Effects

An assemblage of diagnostic shock effects are observed within the parautochthonous rocks of the structure's center, floor (below the allochthonous fill), and walls. These include shatter cones, planar microstructures including PDFs, diaplectic glass, and selective mineral melting.

Shatter Cones

Numerous studies (e.g., Milton 1977; Roddy and Davis 1977) have shown that shatter cones are diagnostic of peak shock pressures in the range of approximately 2–25 GPa. Poorly developed shatter cones occur broadly within the target rocks of the Terny structure and are best developed in PR_1kr_2 schists and gneisses. Shatter cones in surface and subsurface exposures typically are 15–20 cm long and expose 20–40° of the cones circumference (Fig. 5e).

Abundant shatter cones occur in the surface exposures within parautochthonous target rocks in the northwestern section of the Pervomaysk quarry and—most notably—along the southern margin of the Annovsk open pit (prominent locations denoted by S in Fig. 3). The Pervomaysk cones point up 15–45° from horizontal and in the northwestward direction whereas those in the Annovsk pit are shallowly inclined toward the south. We observed shatter cones within the walls of mining level 750 m (Fig. 3) at locations corresponding to the crater floor beneath the breccia-filled annular trough; these cones generally point upward in a westward direction at 15–60° with inclinations generally decreasing with distance away from P2.

Planar Microstructures Indicative of Shock Deformation

Planar microstructures include planar fractures and PDFs that have been produced by hypervelocity shock damage to the mineral grain (Stöffler and Grieve 2007). PDFs in quartz are one of the most reliable and clearly distinguishable indicators of shock metamorphism. Aside from some hydrothermal quartz veins that postdate the impact, all our samples of quartz-bearing rocks of the Kryvoriz'ka series located in the central zone of parautochthonous rocks that contain planar fractures and PDFs in quartz grains. In addition to undulatory extinction (Figs. 6a–d), quartz typically shows multiple sets (up to 5) of PDFs apparent in thin section (Figs. 6e–g).

We derived peak shock pressures from quartz grains (e.g., Figs. 6e–i) showing minimal undulosity in selected thin sections from parautochthonous target samples by first measuring the angle between the pole to each PDF and the grain's optical axis using a 4-axis universal stage. These angles were then compared with angles predicted for rational Miller indices indicative of crystallographic orientations (Stöffler and Langenhorst 1994). A variety of studies on naturally shocked quartz from terrestrial structures have shown that PDF orientation is indicative of the peak shock pressure the sample has experienced (von Engelhardt and Stöffler 1968; Robertson et al. 1968; von Engelhardt and Bertsch 1969) and shock recovery experiments have indexed these orientations to specific shock pressure ranges (e.g., Stöffler 1984; Stöffler and Langenhorst 1994). For our analysis, we use the shock pressure values provided in French and Koeberl (2010, section
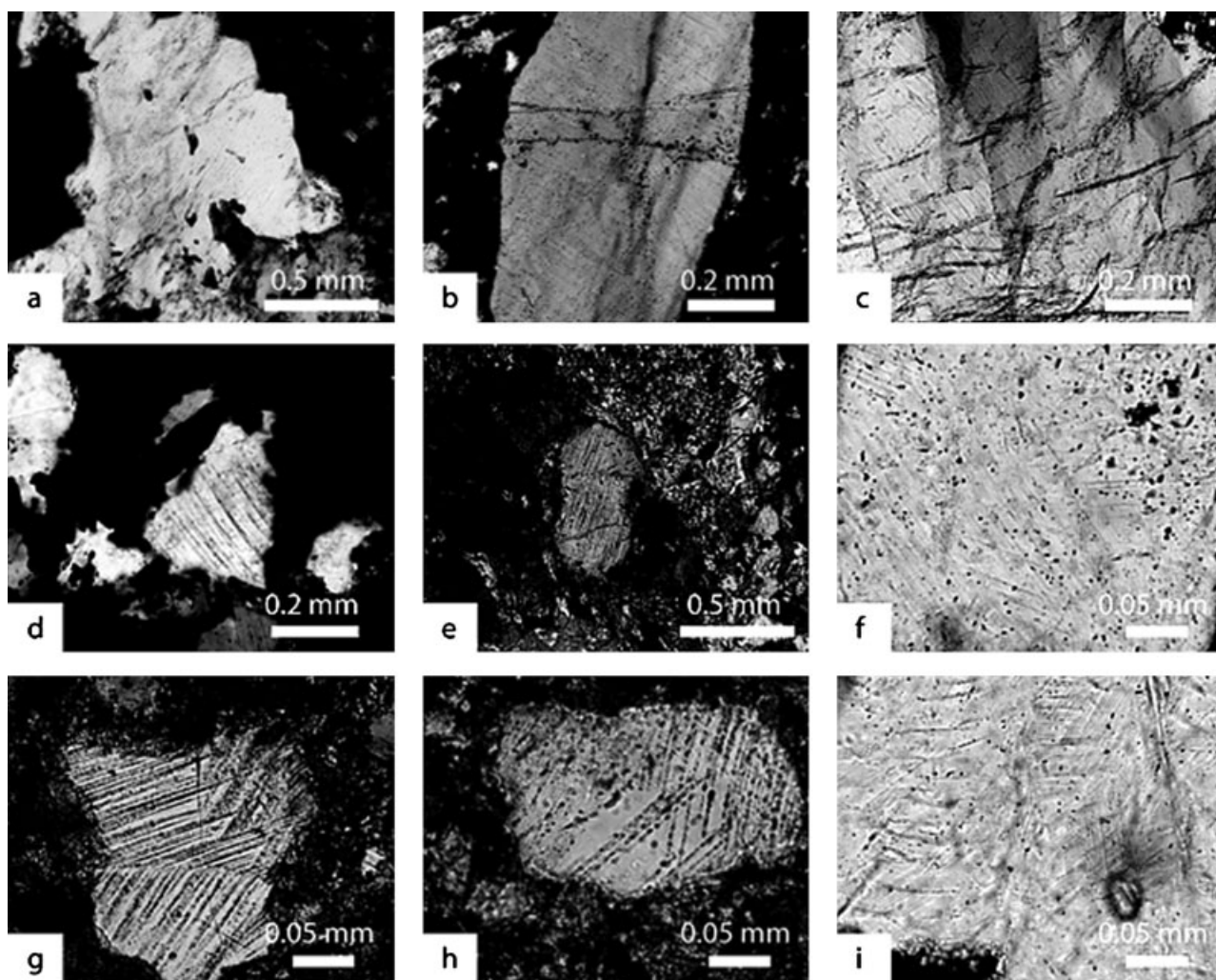
Fig. 6. Shocked quartz grains from the Terny impact structure. a) Quartz grain showing some wavy extinction, crossed polars; b, c) quartz grain with wavy extinction and visible basal [0001] PDF, crossed polars; d) basal planar fracture in quartz grain from magnetite quartzite, crossed polars; e) heavily shocked quartz crystal from allochthonous breccia, PDF system is clearly visible, crossed polars; f) quartz crystal with three sets of PDF, plain light; g) heavily shocked quartz grain from allochthonous breccia, crossed polars; h) quartz grain from parauthochtonous breccia carrying two systems of decorated PDF, crossed polars; i) multiple PDFs in quartz from allochthonous breccia, plain light.

3.3). Where a range of pressures is given, we have used the median value.

We observed no planar microstructures from any sampled subsurface level within approximately 0.5 km of the United shaft. Beyond this point, toward the P1-P2 complex, subsurface samples of parautochthonous rocks immediately adjacent to the crater-fill deposit exhibit quartz grains with abundant planar fractures with polar angles of approximately 0° and approximately 52°, indicative of "c" (0001) and "r" {10$\bar{1}$1} (or "z" {01$\bar{1}$1}) Miller indices, respectively. In addition, approximately 20% of the grains in these samples contain PDFs oriented parallel to the basal plane (0001). These planar microstructures indicate shock pressures in the range of 5–10 GPa (French and Koeberl 2010).

Nearer to the P1 and P2 mine shafts (Figs. 3, 4), the frequency of shocked quartz grains increases. At about 2 km east and south of P1, 50–100% of quartz grains exhibit 2–5 sets of PDFs with trapezoidal, i.e., "ω" {10$\bar{1}$3} orientations most common. Planar elements in those crystals commonly are decorated with small (<10 μm) bubbles. In some of these crystals PDFs are visible only at higher magnification (Fig. 6i). Shock recovery experiments and other shock barometry studies (e.g., Robertson et al. 1968; Stöffler 1984; Stöffler and Langenhorst 1994) indicate that trapezoidally oriented PDFs are characteristic of shock levels in the range of about 12 GPa.

Melt rocks from the P1 and P2 shafts have but a few unaffected quartz grains remaining and distinct
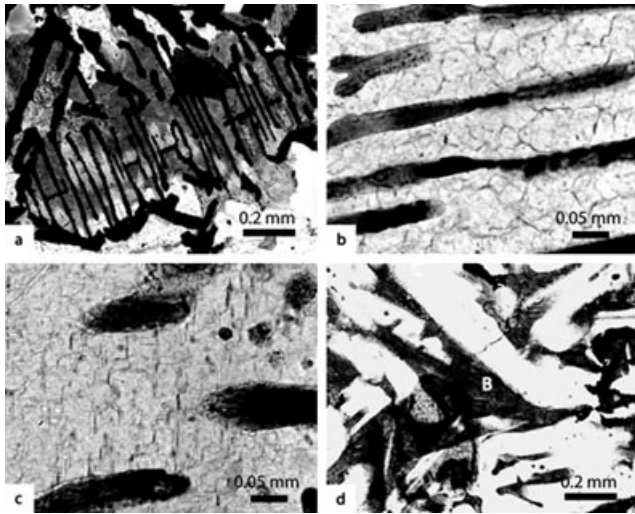
Fig. 7. Highly shocked diaplectic glass and selective melting of magnetite in thin section: a) a cross cut of magnetite skeletal crystal (20×, plain light), a signature of fast growth after shock release; b) rounded anhedral chlorite replacing original biotite in quartz-bearing fragment having undergone impact-induced vitrification followed by recrystallization (indicated by ballen structures); c) remains of PDFs in diaplectic quartz glass exhibiting ballen-like microstructures; d) secondary chlorite over biotite (B).

evidence of planar deformation features is not common. Planar elements can be obscured by secondary minerals especially in rocks that have sustained high temperatures and associated hydrothermal effects over an extended period of time.

Diaplectic Glass and Selective Mineral Melting

Shock-produced diaplectic glasses (Stöffler 1972, 1984) exhibiting the original habit of the parent crystal were observed and sampled in the northwestern edge of Pervomaysk quarry and in subsurface exposures. Figure 7 shows photomicrographs of a biotite-magnetite quartzite with skeletal magnetite crystals (Fig. 7a) in which much of the sample has been converted into glass. Both quartz and biotite have rounded anhedral edges (Fig. 7b). Even though quartz shows partial isotropization, remnant PDFs are evident within the nonvitrified portions of the grain (Fig. 7c). Although biotite grains are heavily chloritized (Fig. 7d), some unaltered cores remain and these are also optically isotropic. These observations indicate that, prior to its alteration, this sample experienced shock pressures in the range of approximately 40 GPa (French and Koeberl 2010) that resulted in partial isotropization of quartz and biotite and selective melting of magnetite.

Synthesis

The distribution of shock indicators presented above indicates that peak shock pressures drop from 40 GPa (outward extent of diaplectic quartz glass) to 2 GPa (outward extent of shatter cones). In the northwest corner of the Pervomaysk quarry peak pressures appear to drop toward the center of the quarry, or approximately in a southeastward direction. We observed this eastward decline in peak pressure in subsurface mine walls at levels 365 and 520 m beginning approximately 800 m to the east of the P2 shaft. Safety concerns prohibited us from determining if the pressure gradient was observable at deeper mine levels. Nonetheless, we have constrained the location of the 40 GPa isobar in two widely separated locations. Because peak shock pressure decays radially from the impact point, this provides an important constraint to locating the impact site (crater center), as discussed in the following section.

RECONSTRUCTING THE TERNY IMPACT CRATER

Virtually all terrestrial impact structures whose diameters are greater than a few kilometers have been severely modified by subsequent surface activity (e.g., Grieve and Shoemaker 1994). Erosion, while providing the benefit of exposing substructure to observation, modifies or completely erases the cardinal shape characteristics that define fresh craters on airless bodies such as the Moon. Sedimentary infilling provides a stratigraphic age constraint on the impact event but also obscures the structure from direct observation. Consequently, efforts to reconstruct the original morphological characteristics of large terrestrial structures are met with considerable, sometimes insurmountable challenges.

Craters formed in crystalline targets pose an additional challenge. Unlike layered sedimentary assemblages, igneous and metamorphic complexes do not typically form or retain systematic, lithologically distinct horizons from which a reliable stratigraphic framework can be derived. It is not possible therefore to measure the displacements that rocks in various crater units have undergone from their pre-impact positions. This severely limits ability to reconstruct such important characteristics as the amount of uplift on rocks of the central structure, excavation depth, and fault throw. And without recognizable layering, seismic profiling is of limited utility.

Location and Transient Crater Diameter

Determinations of the original size and center location of the Terny crater are inexorably linked because only a small portion of the structure has been adequately explored. Occurrences of solid-state

indicators of shock metamorphism, including shatter-cone localities, clearly indicate that the two open-pit mines bracket the impact site to the north and south, requiring the structural center to lie on an E–W trending line located within a 2 km wide zone bounded by 48.127° N and 48.145° N.

The shock pressure distribution derived from our sample analyses indicates that the geographic center of Terny lies to the west of the P1, P2 mine shafts but the distance westward is not well constrained. The remains of the allochthonous crater fill (Fig. 3) form an arcuate deposit exposed within the Pervomaysk open pit and are also exposed within the walls of subsurface mine levels between the P1, P2, and United shafts. By assuming radial symmetry of this deposit and constraining its outward margin to be southward of the Annovsk pit (where allochthonous breccias are not observed), we derive the concentric structure shown in Fig. 3, with the geographic center point at 48.130° N; 33.520° E (A; Fig. 3). This interpretation is consistent with the location of the 40 GPa shock isobar we have observed and units defined on the unpublished industrial map that we have updated (Fig. 4). Specifically, our derived center location places the oldest (i.e., deepest) unit in the center of the uplift and the clastic dyke-filled megablock zones along the uplift margins.

The model presented in Figs. 3 and 4 assumes that both the allochthonous crater-fill deposits and the 40 GPa shock isobar are circular and perfectly concentric. It is well known that effects such as oblique impact trajectory, target heterogeneity, and differential erosion can result in impact structures that deviate considerably from this ideal form. Nonetheless, it is unlikely that the crater center lies eastward of point A (Fig. 3) for the reasons given above; however, the coarse granularity of observations allow the center to be located up to approximately 1 km southwest of A. This would enlarge the rings shown in Figs. 3 and 4 and result in a somewhat larger estimate of Terny's diameter. We prefer the point A location, however, as it is consistent with all available observations and results in a conservative estimate of the original size of the Terny crater. In any event, given this structure's poor exposure, a more precise and reliable estimate is not attainable.

Fig. 8 plots the maximum distance from point A that each of the diagnostic shock features were observed against the pressure it indicates. The dashed line connects the two points we have the most confidence in: the outward limit of samples containing diaplectic glass and the outward extent of shatter cones in parautochthonous target rocks, both collected from surface exposures. The points indicating isobars derived
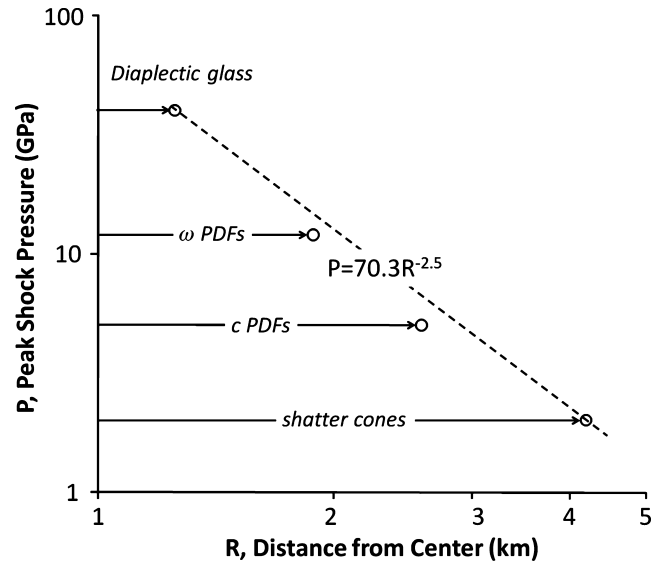

Fig. 8. Radial distribution of shock pressures observed within the Terny structure. Open circles denote the maximum observed distance from the estimated crater center for each of the four shock pressure indicators. Because of limitations in precisely locating the maximum distances of PDFs (discussed in the text), the power law relating peak pressure P to radial distance R was derived by fitting the outward extents of diaplectic glasses and shatter cones.

from PDF orientations were collected from subsurface exposures at a depth of 520 m. Sample access at this level was severely limited and we are not able to confidently locate the outward extent of the shock isobars that these PDFs indicate.

Theoretical and observationally based models of shock attenuation at complex craters (e.g., Dence et al. 1977; Robertson and Grieve 1977; Kieffer and Simonds 1980) indicate that peak shock pressure P attenuates with radial distance, R, as $P \propto R^{\xi}$, where best estimates of ξ range from -3 to -5.5 (Dence et al. 1977; Robertson and Grieve 1977; Kieffer and Simonds 1980). The power law we show in Fig. 8 ($P = 70.3R^{-2.5}$) is our best estimate of the peak shock pressure distribution along the true crater floor (i.e., below the breccia lens) of the eroded Terny impact structure. It is expected that the attenuation rate here will be shallower than predicted radial attenuation rate because the rocks preserved in the crater center do not represent a radial transect from the origin of the shock front. Instead, the crater floor consists of rocks that were originally well below the "effective depth of burst" (e.g., Melosh 1980) and have been uplifted during late-stage collapse and are thus shocked to lower pressures than those vaporized, melted, and/or ejected from nearer the impact point.

Armed with a reasonable shock attenuation rate, determination of the diameter of the original Terny
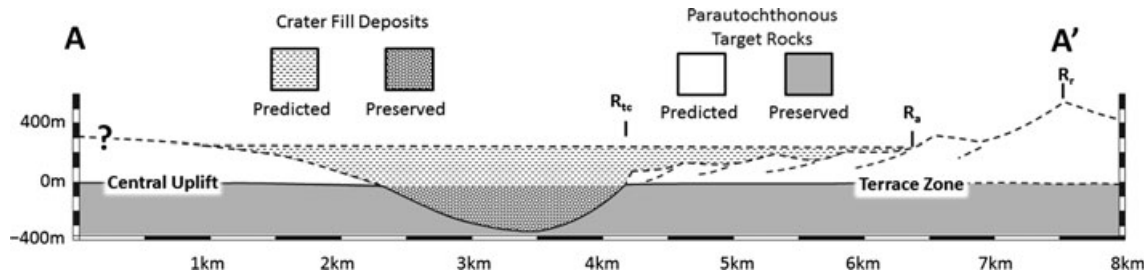
Fig. 9. Reconstructed cross section of the pristine Terny impact crater based on observations discussed in the text, appropriate scaling relationships, and comparison with the similarly sized El'gygytgyn crater. Dimensions are based on a 6.5 km apparent crater radius (R_a) for Terny and a 7.5 km R_a for El'gygytgyn (Collins et al. 2008). Consequently, all relevant morphometric features have been scaled to 0.85 El'gygytgyn values. R_{tc} represents the estimated transient crater rim based on shatter-cone occurrences; R_r indicates the calculated location of the crater rim. Table 3 summarizes derived dimensions. Dashed lines indicate predicted (simplified) surfaces. No vertical exaggeration.

crater rests on assumptions about the transient crater boundary. Kieffer and Simonds (1980) propose that the rim of the transient crater is defined by a peak shock pressure of 0.2 GPa, whereas Dence et al. (1977) prefer 2.0 GPa. This order of magnitude range in possible rim pressures poses a severe challenge to reconstructing the original dimensions of severely eroded craters. We note, however, that reconstructions of other such craters have relied principally on the 2.0 GPa estimate (Dence et al. 1977; Robertson and Grieve 1977). In estimating the size of the Terny transient crater, we also rely on the 2.0 GPa isobar for consistency with the existing cratering record. Under this assumption, we derive a radius of approximately 4.2 km for the transient (or excavation) crater.

Final Diameter, Original Morphology, and Preservation State

Using a variety of observational constraints gathered from terrestrial crater studies, Grieve et al. (1981) derived a scaling relationship linking the diameter of the final (apparent) crater, D_a and its zone of deep excavation D_e, such that $D_e = 0.5–0.65\ D_a$. Assuming that D_e is more or less equivalent to the transient crater boundary, the apparent diameter of the Terny impact crater would have been 13–14.5 km as measured from the pre-impact surface.

This D_a estimate places the Terny crater close in size to the 18 km diameter El'gygytgyn crater (Gurov and Koeberl 2004) in Siberia, which has an apparent diameter of 15 km as summarized in Collins et al. (2008). Because El'gygytgyn crater is one of Earth's best-preserved complex impact craters and one that, like Terny, was produced in a crystalline target-rock assemblage, it provides the most reliable means possible of reconstructing additional details of how the Terny crater appeared shortly after its formation.

In the radial cross section presented in Fig. 9, we use the conservative estimate of Terny's apparent diameter, $D_a = 13$ km, and assume that the pristine Terny crater was morphologically proportional to El'gygytgyn to derive rim height, rim radius, and the thickness of the crater fill. For this, we rely on the observed values of El'gygytgyn presented in table 1 of Collins et al. (2008). While this morphometric scaling provides a reasonable basis for deriving Terny's original dimensions, it is not without limitations and our model results should be used with caution. For instance, Terny's central uplift is approximately 4 km wide if measured from the edge of the preserved allochthonous deposits (or approximately 7 km wide if measured from the bottom of the peripheral trough) whereas seismic data at El'gygytgyn indicate that the central uplift there is only approximately 2 km in diameter (Gebhardt et al. 2006). Important morphological variations in fresh craters of comparable size are common on the Moon and other airless bodies within the solar system. This uplift apparently is not exposed as a central peak at El'gygytgyn (Niessen et al. 2007) and it is unclear whether or not the uplift at Terny protruded above the crater-fill deposits either.

Given that the allochthonous deposits at Terny reach a maximum thickness of about 360 m, and our calculated apparent depth is approximately 550 m, erosion has removed no more than approximately 200 m of the crater-fill deposits. Adding in the model rim height (120 m) indicates that the total erosion the Terny crater has experienced is approximately 320 m.

CONCLUDING REMARKS

Table 3 summarizes the relevant geographic and morphometric characteristics we have derived from our analysis of the Terny structure. These values represent the most consistent and conservative estimates currently

Table 3. Preferred estimates of basic morphological properties of the reconstructed Terny crater.

		Notes
Center location	48.130° N; 33.520° E	Yields minimum crater size
Transient crater diameter, D_{tc}	8.4 km	Center location to limit of shatter cones
Apparent crater diameter, D_a	13 km (up to ~17 km)	D_{tc} = 0.5–0.65 Da
Rim diameter, D_r	15.6 km (up to ~19 km)	0.87 D_r (El'gygytgyn)
Rim height, H_r	~120 m	0.87 H_r (El'gygytgyn)
Apparent depth, D_a	~550 m	0.87 D_a (El'gygytgyn)
Width of exposed rim zone, W_r	~1.3 km	0.87 $D_r - D_a$ (El'gygytgyn)
Width of central uplift, W_u	~7 km	Measured from location of maximum breccia thickness
Thickness of allochthonous breccia removed by erosion, T_e	~200 m	D_a (Terny) minus thickness of preserved breccia.
Total relief lost by erosion	~320 m	$T_e + H_r$

possible and supplant previous estimates such as those in Table 1.

As previously noted, crater reconstructions of poorly exposed, deeply eroded impact structures are difficult and exceedingly so for structures in crystalline rocks. Thus, comprehensive reconstructions such as the one presented here are exceptionally rare. Consequently, relating the structural elements exposed in terrestrial structures to the morphological features commonly observed in fresh craters on planets throughout the solar system is one of the fundamental remaining challenges of impact studies. With Terny's array of surface and surface exposures as well as its apparent morphological similarities to the well-preserved El'gygytgyn crater, additional attention and effort to evaluate Terny could be significant in bridging this gap.

Editorial Handling—Dr. Gordon Osinski

REFERENCES

Bibikova E. V., Lobach-Zhuchenko S. B., Artemenko G. V., Claesson S., Kovalenko A. V., and Krylov I. N. 2008. Late Archean magmatic complexes of the Azov terrane, Ukrainian Shield: Geological setting, isotopic age, and sources of material. *Petrology* 16:211–231.

Collins G. S., Kenkmann T., Osinski G. R., and Wünnemann K. 2008. Mid-sized complex crater formation in mixed crystalline-sedimentary targets: Insights from modeling and observation. *Meteoritics & Planetary Science* 43:1955–1977.

Dence M. R., Grieve R. A. F., and Robertson P. B. 1977. Terrestrial impact structures: Principal characteristics and energy considerations. In *Impact and explosion cratering*, edited by Roddy D. J., Pepin R. O., and Merrill R. B. New York: Pergamon Press. pp. 247–275.

Engelhardt W. von. 1997. Suevite breccia of the Ries impact crater, Germany: Petrography, chemistry and shock metamorphism of crystalline rock clasts. *Meteoritics & Planetary Science* 32:545–554.

Engelhardt W. von. and Bertsch W. 1969. Shock induced planar deformation features in quartz from the Ries crater, Germany. *Contributions to Mineralogy and Petrology* 20:203–234.

Engelhardt W. von. and Stöffler D. 1968. Stages of shock metamorphism in crystalline rocks of the Ries Basin, Germany. In *Shock metamorphism of natural materials*, edited by French B. M. and Short N. M. Baltimore, Maryland: Mono Book Corp. pp. 229–295.

Eremenko G. K. and Yakovlev V. M. 1980. Terny astrobleme in North Kryvyj Rig region. *Reports of Academy of Science of USSR* 2:449–451.

French B. M. and Koeberl C. 2010. The convincing identification of terrestrial meteorite impact structures: What works, what doesn't, and why. *Earth-Science Reviews* 98:123–170.

Gebhardt A. C., Niessen F., and Kopsch C. 2006. Central ring structure identified in one of the world's best preserved impact craters. *Geology* 34:145–148.

Grieve R. A. F. 1982. The record of impact on Earth: Implications for a major Cretaceous-Tertiary impact event. *Geological Society of America Special Paper* 190:25–37.

Grieve R. A. F. 1987. Terrestrial impact structures. *Annual Review of Earth and Planetary Sciences* 15:245–270.

Grieve R. A. F. and Masaitis V. L. 1994. The economic potential of terrestrial impact craters. *International Geology Review* 36:105–151.

Grieve R. A. F. and Robertson P. B. 1979. The terrestrial cratering record. *Icarus* 38:212–229.

Grieve R. A. F. and Shoemaker E. M. 1994. The record of past impacts on Earth. In *Hazards due to comets and asteroids*, edited by Gehrels T. Tucson, Arizona: The University of Arizona Press. pp. 417–467.

Grieve R. A. F., Robertson P. B., and Dence M. R. 1981. Constraints on the formation of ring impact structures based on terrestrial data. In *Multi-ring basins: Formation and evolution, Proceedings of Lunar and Planetary Science*

12A, edited by Schultz P. H. and Merrill R. B. New York: Pergamon. pp. 37–57.

Grieve R. A. F., Rupert J., Smith J., and Therriault A. 1995. The record of terrestrial impact cratering. *GSA Today* 5:189–196.

Gurov E. P. 1982. Stishovite from the Terny astrobleme. *Mineralogical Journal* 4:75–76.

Gurov E. P. and Koeberl C. 2004. Shocked rocks and impact glasses from the El'gygytgyn impact structure, Russia. *Meteoritics & Planetary Science* 39:1495–1508.

Kieffer S. W. and Simonds C. H. 1980. The role of volatiles and lithology in the impact cratering process. *Reviews of Geophysics and Space Physics* 18:143–181.

Krochuk R. V. and Sharpton V. L. 2003. Morphology of the Terny astrobleme based on the field observation and sample analysis (abstract #1489). 34th Lunar and Planetary Science Conference. CD-ROM.

Masaitis V. L. 1999. Impact structures of northeastern Eurasia: The territories of Russia and adjacent countries. *Meteoritics & Planetary Science* 34:691–711.

Masaitis V. L., Mashchak M. S., and Ezersky V. A. 1981. High-ferruginous tagamites from the Terny astrobleme (Ukrainian shield) (abstract). 12th Lunar and Planetary Science Conference. p. 655.

Mashchak M. S. and Orlova Z. V. 1985. Recrystallized diaplectic quartz from the Ternovskaya astrobleme. *Meteoritika* 44:164–167. (In Russian)

Melosh H. J. 1980. Cratering mechanics—Observational, experimental, and theoretical. *Annual Review of Earth and Planetary Sciences* 8:65–93.

Milton D. J. 1977. Shatter cones—An outstanding problem in shock mechanics. In *Impact and explosion cratering*, edited by Roddy D. J., Pepin R. O., and Merrill R. B. New York: Pergamon Press. pp. 703–714.

Mordovets L. F. 1977. Subvolcanic sienite-trachiandesite complex rocks of north Kryvyj Rig area. *Geochemistry and Ore Formations* 6:42–46.

Niessen F., Gebhardt A. C., Kopsch C., and Wagner B. 2007. Seismic investigation of the El'gygytgyn impact crater lake (Central Chukotka, NE Siberia): Preliminary results. *Journal of Paleolimnology* 37:49–63.

Nikol'sky A. P. 1979. On the genesis of tridimite-hizingerite rocks from Pervomaysk deposit in Krivoy Rog. *Reports of Academy of Science of USSR* 249:436–439. (In Russian)

Nikol'sky A. P. 1991. *Geology of Pervomaysk iron deposit and meteorite impact influence on its structure*. Moscow: Nedra, Ministry of Geology, USSR. 71 p. (In Russian)

Nikol'sky A. P., Naumov V. P., and Korobko N. I. 1983. Pervomaysk iron-ore deposit in the Krivoy Rog and its transformation by impact metamorphism. *International Geology Review* 25:1304–1315.

Reimold W. U., Koeberl C., Gibson R. L., and Dressler B. O. 2005. Economic mineral deposits in impact structures: A review. In *Impact tectonics*, edited by Koeberl C. and Henkel H. Berlin: Springer. pp. 479–552.

Robertson P. B. and Grieve R. A. F. 1977. Shock attenuation at terrestrial impact craters. In *Impact and explosion cratering*, edited by Roddy D. J., Pepin R. O., and Merrill R. B. New York: Pergamon Press. pp. 687–702.

Robertson P. B., Dence M. R., and Vos M. A. 1968. Deformation in rock-forming minerals from Canadian craters. In *Shock metamorphism of natural materials*, edited by French B. M. and Short N. M. Baltimore, Maryland: Mono Book Corp. pp. 433–452.

Roddy D. J. and Davis L. K. 1977. Shatter cones formed in large-scale experimental explosion craters. In *Impact and explosion cratering*, edited by Roddy D. J., Pepin R. O., and Merrill R. B. New York: Pergamon Press. pp. 715–750.

Shcherbak N. P., Bartnitsky Y. N., Bibikova E. V., and Boyko V. L. 1984. Age and evolution of the Early Precambrian continental crust of the Ukrainian Shield. In *Archaean geochemistry: The origin and evolution of the Archaean continental crust*, edited by Kröner A. Berlin: Springer. pp. 251–261.

Stöffler D. 1972. Deformation and transformation of rock-forming minerals by natural and experimental shock processes: I. Behavior of minerals under shock compression. *Fortschritte der Mineralogie* 49:50–113.

Stöffler D. 1984. Glasses formed by hypervelocity impacts. *Journal of Non-Crystalline Solids* 67:465–502.

Stöffler D., and Grieve R. A. F. 2007. Impactites. In *Metamorphic rocks: A classification and glossary of terms, recommendations of the International Union of Geological Sciences*, edited by Fettes D. and Desmons J. Cambridge: Cambridge Press. pp. 1–30.

Stöffler D., and Langenhorst F. 1994. Shock metamorphism of quartz in nature and experiment: I. Basic observation and theory. *Meteoritics* 29:155–181.

Val'ter A. A. 1992. *Shock–metamorphogenic carbon minerals.* Kiev: Naukova Dumka. 170 p. (In Russian)

Val'ter A. A. and Ryabenko V. A. 1982. Ternovskaya astroblema; Krivoy Rog. In *The geology and petrology of meteorite craters*, edited by Ryabenko V. A. Kiev, USSR: Izd. Nauk. Dumka. pp. 193–202. (In Russian)

Val'ter A. A., Ryabenko V. A., and Kotlovskaya F. I. 1981. The Ternovka astrobleme: New and most deeply eroded meteorite crater on the Ukrainian shield. *Doklady Akademii Nauk SSSR* 2:3–7. (In Russian)

Val'ter A. A., Kolesov G. M., Sapozhnikov D. Y., and Miklishansky A. Z. 1989. The distribution of meteoritic material in impactites from the Terny astrobleme (Krivoi Rog, Ukraine). 20th Lunar and Planetary Science Conference. pp. 1148–1149.